Changes in Arctic sea ice result in increasing light transmittance and absorption

M. Nicolaus,[1] C. Katlein,[1] J. Maslanik,[2] and S. Hendricks[1]

[1] Arctic sea ice has declined and become thinner and younger (more seasonal) during the last decade. One consequence of this is that the surface energy budget of the Arctic Ocean is changing. While the role of surface albedo has been studied intensively, it is still widely unknown how much light penetrates through sea ice into the upper ocean, affecting sea-ice mass balance, ecosystems, and geochemical processes. Here we present the first large-scale under-ice light measurements, operating spectral radiometers on a remotely operated vehicle (ROV) under Arctic sea ice in summer. This data set is used to produce an Arctic-wide map of light distribution under summer sea ice. Our results show that transmittance through first-year ice (FYI, 0.11) was almost three times larger than through multi-year ice (MYI, 0.04), and that this is mostly caused by the larger melt-pond coverage of FYI (42 vs. 23%). Also energy absorption was 50% larger in FYI than in MYI. Thus, a continuation of the observed sea-ice changes will increase the amount of light penetrating into the Arctic Ocean, enhancing sea-ice melt and affecting sea-ice and upper-ocean ecosystems. **Citation:** Nicolaus, M., C. Katlein, J. Maslanik, and S. Hendricks (2012), Changes in Arctic sea ice result in increasing light transmittance and absorption, *Geophys. Res. Lett.*, *39*, L24501, doi:10.1029/2012GL053738.

1. Introduction

[2] During the last years, a change towards a smaller [*Serreze et al.*, 2007], younger [*Comiso*, 2012; *Maslanik et al.*, 2011; *Maslanik et al.*, 2007] and thinner [*Haas et al.*, 2008; *Kwok and Rothrock*, 2009] sea-ice cover in the Arctic has been observed. Arctic sea ice was mainly composed of old multi-year sea ice (MYI) in the 1980's and 1990's. However, since 2008, the amount of this old, thick ice has decreased. Summer sea ice is now composed of at least 50% first-year sea ice (FYI), while sea ice older than 4 years has been almost completely lost (<10% in September 2011). This trend towards younger and more seasonal sea ice also implies that the ice cover is getting thinner, less snow covered, saltier, less deformed, and more fragile. These changes affect the optical properties of sea ice, reducing its ability to reflect light back to the atmosphere and increasing its transparency towards the ocean [*Perovich et al.*, 2011]. Over the last decades, a comprehensive understanding of the interaction of solar short-wave radiation (light) with sea ice and its snow cover has been developed, resulting in parameterizations for different ice types and seasons [*Perovich*, 2005; *Perovich and Polashenski*, 2012]. Based on this, estimates of solar heat input into the Arctic Ocean reveal a trend towards more heat input through more open water and earlier melt onset [*Perovich et al.*, 2011]. Hence, it can be concluded that light transmission into the ocean will increase for areas that become (seasonally) ice-free. But how much light is transmitting through sea ice, and how might that change in future? This question is of critical importance for the sea-ice energy and mass balances, and the fresh-water budget of the upper ocean.

[3] One of the most challenging questions in Arctic marine ecology is how primary productivity will change due to changing sea ice covers [*Arrigo et al.*, 2008, 2012]. This question is highly related to the availability of light (and nutrients), the main energy source for primary productivity, the basis of all life in the ice covered Arctic Ocean [*Popova et al.*, 2012]. Also the horizontal and vertical distributions of light play a key role for geo-chemical processes, e.g. photo-oxidization. Despite this interdisciplinary interest in light transmission through sea ice, no large-scale estimate of light penetration through sea ice has yet been available. As a result, all (ecosystem) models are based on rough estimates based on a few spot measurements. The main reason is the lack of consistent and comprehensive field measurements, which are technically and logistically challenging. Such observations need to capture the considerable horizontal and vertical variability that results from the heterogeneous and seasonally changing sea ice cover. Only recently, more attempts have been realized to increase the amount of time series measurements and transects of under-ice radiation [*Ehn et al.*, 2011; *Nicolaus et al.*, 2010b]. Here we present the first large-scale data set of under-ice radiation in the central Arctic, collected using spectral radiometers on a remotely operated vehicle (ROV) [*Nicolaus and Katlein*, 2012]. Our analyses result in a simple parameterization of light transmission through ponded and white FYI and MYI. Applying this parameterization to satellite observations allowed us to derive Arctic-wide estimates of under-ice light conditions.

2. Methods

2.1. In-Situ Measurements and Observations

[4] All measurements were performed during the transpolar cruise ARK-XXVI/3 (TransArc, 2011, Figure 1) of the German ice breaker RV Polarstern. Spectral radiation measurements were performed with Ramses spectral radiometers (Trios GmbH, Rastede, Germany) operated under sea ice on a V8Sii ROV (Ocean Modules, Åtvidaberg, Sweden). All under-ice radiation data were corrected to the ice-ocean

---

[1]Alfred Wegener Institute for Polar and Marine Research, Bremerhaven, Germany.

[2]Department of Aerospace Engineering Sciences, University of Colorado Boulder, Boulder, Colorado, USA.

Corresponding author: M. Nicolaus, Alfred Wegener Institute for Polar and Marine Research, Bussestrasse 24, DE-27570 Bremerhaven, Germany. (marcel.nicolaus@awi.de)
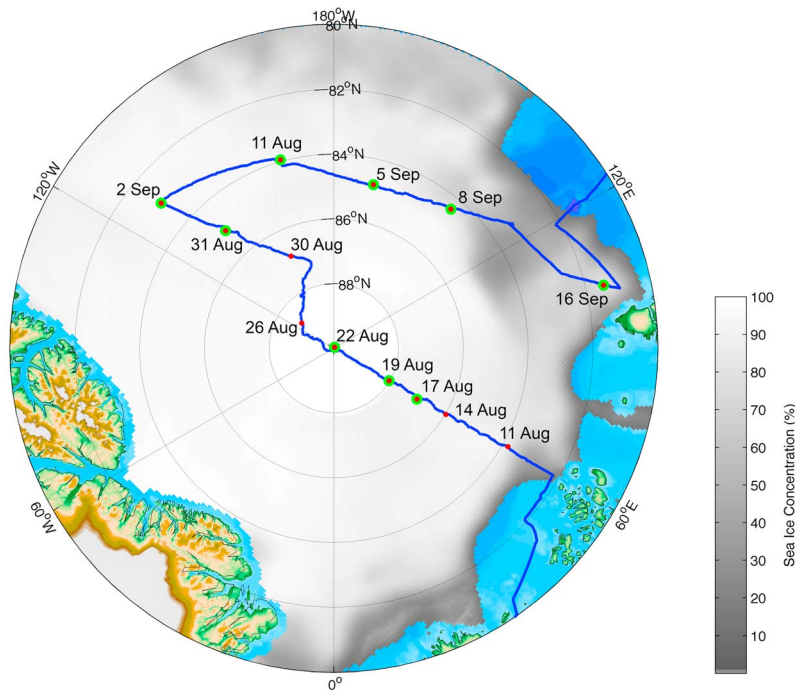
Figure 1. Cruise track (blue line) with ROV stations (green dots) and ice stations (red dots) during the expedition ARK-XXVI/3 (TransArc) of the German icebreaker RV Polarstern in summer 2011. The background image shows the mean sea-ice concentration between 10 August and 17 September 2011 as derived from OSI-SAF data.

interface and scaled to the entire range of short-wave radiation (250–2500 nm) for best comparability. In addition to the under-ice measurements, incident solar radiation was measured directly and synchronously at the ROV sites on the sea-ice surface, to enable transmittance calculation. The optical measurements, ROV operations, and data processing are described in detail in *Nicolaus and Katlein* [2012] and *Nicolaus et al.* [2010a]. The ROV was launched through the sea ice at 9 ice stations starting in the Eurasian Basin (17 August), over the North Pole (22 August) into the Canada Basin and towards the last station on the Russian Shelf in the Laptev Sea (16 September). Besides the radiation measurements, sea-ice type (MYI/FYI), sea-ice thickness, snow depth, pond coverage, and surface scattering layer depth were recorded and later assigned to each spectrum. The classification of FYI and MYI was not always obvious, although we also included results from sea-ice core-analyses into the processing. In addition, highly deformed FYI may have pond fractions similar to MYI. And these types can also hardly be distinguished in field observations. Along the entire track, bridge observations of sea ice were performed, following a standardized protocol (ASPeCT) [*Worby et al.*, 2008] adapted for the Arctic.

2.2. Arctic-Wide Up-Scaling

[5] In order to perform the up-scaling analyses, the following data sets were used: (1) SSM/I sea-ice concentration was obtained on a 10 km Polar Stereographic Grid from the Ocean and Sea Ice Satellite Application Facilities (OSI SAF, product ID: OSI-401). (2) The spatial distribution of FYI and MYI was derived from satellite data and Lagrangian time history tracking, using the algorithm of *Maslanik et al.* [2011]. All data were interpolated from their native

12.5-km grid to a 10 km Polar Stereographic Grid, using nearest neighbor resampling. All data points with a valid number for sea-ice concentration but no valid number for ice age were set to FYI. Vice versa, all data without ice concentration were set to open ocean. (3) Surface solar radiation was obtained twice daily from ECMWF Era Interim re-analyses on a 1.5° grid. The data were averaged to daily mean values and interpolated to the 10-km Polar Stereographic Grid, using a triangular cubic interpolation. From all these data sets and the derived parameterization, the solar heat input into the ocean was calculated as

$$E_T(t) = E_S(t) \cdot C(t) \cdot \tau_I + E_S(t) \cdot [1 - C(t)] \cdot \tau_O \qquad (1)$$

with E_T: Transmitted radiation, E_S: Surface solar radiation, C: Sea-ice concentration, and $\tau_{i/o}$: Transmittance of ice or open water (=0.93) [*Pegau and Zaneveld*, 2000]. More details and figures of all used data sets are given in the auxiliary material.[1]

3. Results and Discussion

3.1. Sea-Ice Conditions in Summer 2011

[6] The sea-ice surface consisted of melt ponds and white ice, with the high reflectance of the latter resulting in strongly-scattered solar irradiance. The stations established prior to the North Pole station had open ponds and no snow cover, while surface freezing was observed thereafter. Only the last 3 stations were covered with new snow thicker than 0.05 m. Airborne sea-ice thickness measurements obtained via electromagnetic inductance (EM-bird) along a total

---

[1]Auxiliary materials are available in the HTML. doi:10.1029/2012GL053738.
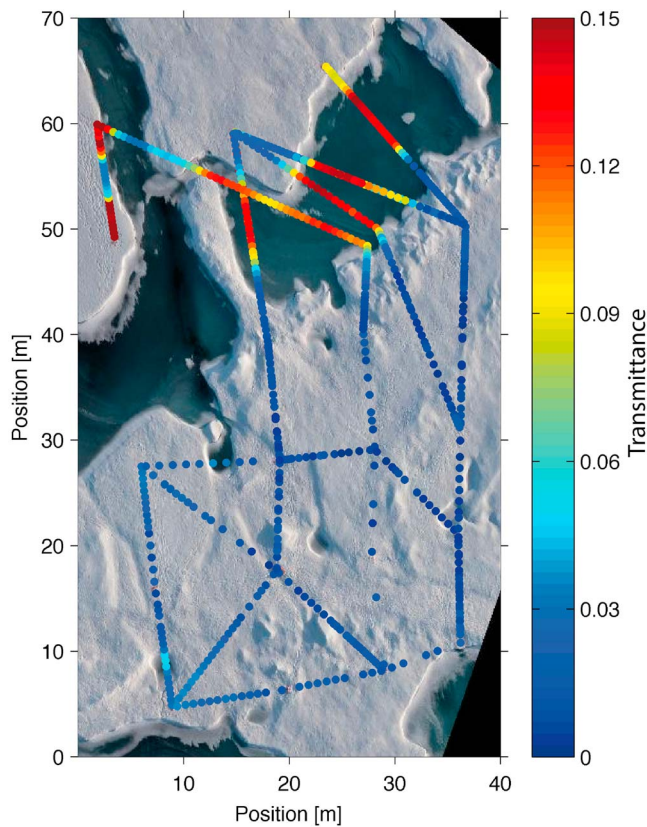
Figure 2. Light (short-wave radiation, 250-2500 nm) transmittance through multi-year sea ice. Results from the ROV measurements on the North-Pole station on 22 August 2011. The background image shows a reference photograph of the ice and pond conditions during measurements. Each colored dot represents one under ice measurement.

length of more than 2500 km resulted in a modal total (snow plus sea ice) ice thickness of 0.9 m, and a mean ice thickness of 1.26 m. The routine sea-ice observations from the bridge show that $42 \pm 10\%$ of the FYI surface was covered by melt ponds, while only $23 \pm 13\%$ of MYI were covered (Figure S1 in the auxiliary material). These results do match the findings of *Fetterer and Untersteiner* [1998], who did find melt-pond concentrations of 30–50% for FYI and 15–25% for MYI from AIDJEX data. The main reason for this are differences in the surface topography of FYI and MYI [*Eicken et al.*, 2004]. FYI surfaces are generally smoother, allowing a wider spread of melt water, resulting in large networks of connected shallow ponds. In contrast, MYI is more deformed and favors more distinct but deeper ponds (see photographs in Figure 3).

[7] Considering the entire Arctic, in August 2011, the sea ice extent was 5.5 Million km^2 with a mean sea-ice concentration of 63%, as observed from passive microwave satellite data (Figure S4). Sea-ice age analyses [*Maslanik et al.*, 2011] reveal that 50% of the sea ice were FYI and 50% were MYI, with MYI dominating along the Greenland and Canada coasts and FYI dominating between 60°E and 150°W (Figure S5). As noted in *Maslanik et al.* [2011], for the data set used, some FYI is likely to be present even in predominantly MYI locations. Hence, the age data to some degree underestimate total area of FYI, so the effects of the transition from a

predominantly MYI pack are likely to be even greater than those described here. Mean solar surface irradiance was 12.3 ± 2.1 Wm^{-2} (Figure S3), with similar fluxes around the mean in the most central Arctic and minima (8.3 Wm^{-2}) in the Barents Sea and maxima in the Laptev Sea (30.1 Wm^{-2}).

3.2. Light Transmission Through FYI and MYI

[8] Under-ice measurements revealed highest fluxes and transmittances under ponded FYI and thin new ice, while much less light transmits through MYI. At the same time, a horizontal variability of one to two orders of magnitude was found on single ice floes of each ice type. This is clearly illustrated in Figure 2, showing the spatial distribution of light transmittance through MYI for the North Pole station on 22 August 2011. At this ice station, sea-ice thickness was 1.5 to 3.0 m, freeboard was 0.2 to 0.4 m, snow depth was <0.01 m, and ice thickness on ponds was <0.05 m. The nadir photograph, taken from a helicopter, shows the distribution of melt ponds and white ice. Each dot represents one light measurement of a grid flown with the ROV under sea ice. Short-wave transmittance ranged from <0.01 to 0.05 for white ice and from 0.08 to 0.20 for ponded ice. This highlights the high contrast between white and ponded MYI, and in particular the variability across the edges between white and ponded ice. Frequency distributions of light transmission through sea ice for this MYI station and the FYI station of 19 August are shown in the Figure S2. Both histograms (FYI and MYI) show distinct modes for ponded and white ice, resulting in light transmittance through Arctic summer sea ice of 0.22 for ponded FYI, 0.04 for white FYI, 0.15 for ponded MYI, and 0.01 for white MYI (Figure 3). These examples are also representative for the entire data set of approx. 6000 under-ice measurements. However, these modes are less dominant in the complete data set since ice conditions varied over the time of the cruise, in particular through snowfall and surface freezing in the later part of the cruise. Therefore, we consider these two stations as most representative for light transmittance through ponded summer sea ice. Reasons for the strikingly higher light transmission through ponds are the missing surface scattering and the thinner ice underlying the ponds [*Eicken et al.*, 2002]. This demonstrates the important role of melt ponds for the surface energy budget and illustrates why they are often considered windows to the ocean.

[9] Including the different fractions of ponded and white ice for both ice types, this results in a total transmittance that is almost threefold greater for FYI (0.11) compared with MYI (0.04) (Figure 3). Applying the same distribution of ponded and white ice for FYI and MYI onto surface albedo [*Perovich*, 1996], we find that FYI has a total albedo of 0.37 while MYI reflects 50% more short-wave radiation, a total of 0.62. This finding was expected and confirms earlier studies [*Perovich and Polashenski*, 2012; *Perovich et al.*, 2011]. But combining these results for albedo and transmittance, we find also that absorption is about 50% larger in FYI (0.52) than in MYI (0.34), favoring a stronger internal warming and melt of sea ice in FYI than in MYI.

3.3. Arctic-Wide Under-Ice Light Distribution

[10] Based on the total transmittance (FYI: 0.11, MYI: 0.04) from the field measurements, and the additional data sets of ice types, ice concentration, and surface solar radiation, an Arctic-wide estimate of light transmission through
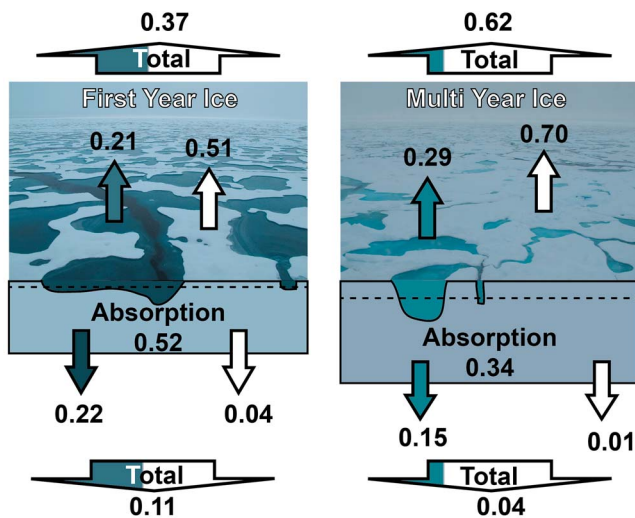
Figure 3. Short-wave albedo, transmittance, and absorption of Arctic first- and multi-year sea ice during summer. Colored arrows refer to melt ponds while white arrows refer to white ice. The pictures show representative photographs of first- and multi-year sea ice. The dashed lines in the sea ice indicate water level. The "Total" arrows average transmittance and albedo over each sea-ice type, considering 23 and 42% ponded surface fractions of multi- and first-year ice, respectively. This fraction is indicated through the colors in the arrows. Albedo for different ice types is taken from *Perovich* [1996]. Absorption is given in the ice as the sum of white ice and ponds.

summer sea ice was derived for August 2011. To do so, E_T (Equation 1) was calculated for each grid cell and each day and averaged over the month. We consider August as the best-represented month from our measurements, when sea ice is covered with open and fully developed melt ponds. Also sea ice conditions are expected to be most consistent over the entire Arctic, because autumn freeze-up has not yet started [*Markus et al.*, 2009]. Figure 4 shows a map of the Arctic-wide distribution of solar heat input through sea ice into the upper ocean, excluding fluxes through open water. This shows an absolute heat input into the ocean between 0 and 2 W m^{-2} for August 2011. Regions with predominant FYI show larger heat input than those with predominating MYI, but the absolute flux is also controlled by surface solar irradiance. Including fluxes through open water, the effect of sea-ice concentration (Figure S4) becomes most obvious, particularly in the marginal ice zones, and fluxes within the sea-ice extent reach more than 5 W m^{-2} (Figure S6). Mean heat flux through the sea ice over the entire Arctic was 0.68 W m^{-2} (mean transmittance: 0.08) in August 2011. Including open water within the sea-ice extent it was 12.3 W m^{-2} (mean transmittance: 0.40).

[11] This bulk approach is different from other estimates of under-ice irradiance [*Light et al.*, 2008] as it is based on direct measurements of above and below ice radiation as well as satellite data. In contrast to radiative-transfer modeling, it is not based on additional assumptions and parameterizations of the sea ice. However, this approach does not allow detailed insights into the optical properties of sea ice on micro scales, which would in turn depend on more detailed and specific measurements. But the presented parameterization seems most useful for large-scale estimates and energy budgets of the
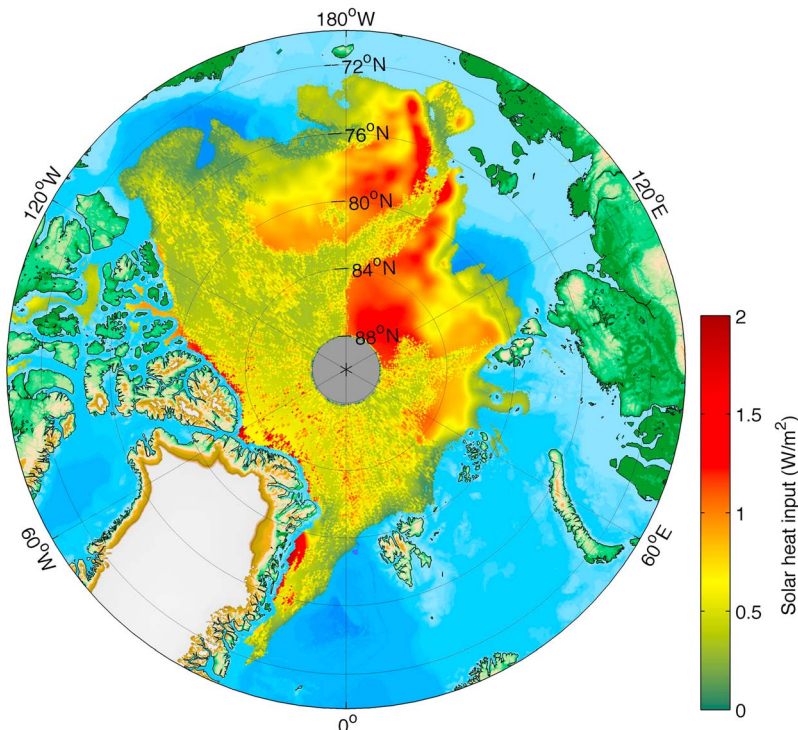
Figure 4. Solar heat input into the Arctic Ocean through sea ice. This map only considers fluxes through sea ice, excluding fluxes through open water, for August 2011.

under-ice environment. It will likely allow using such products to compare with large-scale ocean-ice models [*Gerdes and Lemke*, 2012], in particular those models that include biological and geochemical processes that critically depend on good estimates of under-ice light conditions [*Slagstad et al.*, 2011].

[12] One consequence of the use of these satellite and re-analyses model data is that all the uncertainties and assumptions that are included in these data sets transfer directly into the up-scaling estimates of this study. Other sea-ice concentration and sea-ice type data sets [*Kwok*, 2007] are also available and might yield different results, although such differences are likely to be insignificant for the conclusions presented here. We therefore consider the presented approach to be the best possible estimate at this time, while acknowledging that further improvements of the data products are needed.

3.4. Implications for the Future Arctic

[13] Clearly, short-wave radiative fluxes into the ocean will increase in the future due to sea ice retreat, resulting in more open water. Our results show that there will also be a significant increase of fluxes through the (remaining) sea ice due to the shift to more FYI. To the extent that the FYI measurements described here are representative for today's summer conditions, FYI transmits almost three times as much light as MYI, which is expected to have less and less coverage in the future. Averaging over the entire Arctic with a 50/50 distribution of FYI and MYI in 2011 (Figure S5), today's transmittance of solar irradiance over the entire Arctic sea ice is 0.08. Assuming similar fractions of pond coverage and transmittance ratios of FYI and MYI in the future, solar heat input will increase by about 50% when the point is reached where only small fractions (e.g. 10%) of the Arctic are covered with MYI during summer [*Boé et al.*, 2009]. However, a potential increase of absolute fluxes through sea ice into the upper ocean also depends on the evolution of solar surface irradiance, which is strongly affected by clouds. In addition to the horizontal distribution of light under sea ice, the vertical distribution within the ice column and underlying water will also change depending on ice types, and particularly on melt pond distributions [*Frey et al.*, 2011]. Hence, it may be expected that light penetration into deeper waters will increase accordingly. Beside the consequences for the large-scale energy budget, these changes will strongly impact sea-ice and upper-ocean ecosystems, which depend on light availability for photosynthesis.

[14] Our findings of increased absorption in sea ice also raise the question of how this will affect sea-ice thermodynamics and particularly melt. Would an increased internal absorption be significant for our understanding of how sea ice melts? Increasing absorption would increase internal melt that then becomes even more significant than surface and bottom melt. But in addition, a warmer ocean mixed layer could contribute to stronger basal melt, as well as lower albedo could increase surface melt.

[15] Another aspect that cannot be answered from this study is the question how the trend towards younger MYI within the MYI will affect light transmittance. From the visual field observations it was not possible to distinguish second-year from older sea ice. Even the classification of FYI and MYI has to be considered the greatest uncertainty in this study, although we are confident that the large numbers of observations compensate for most of these effects. In that respect, strongly deformed FYI is also much more similar to

MYI than level FYI. Hence, changes in sea-ice dynamics could also impact light transmittance of future sea ice beyond the here presented aspects.

3.5. Seasonality of Light Transmission

[16] The presented study only covers late summer conditions, because this is the only time of the year where this kind of ROV based measurements exist to our knowledge. It therefore seemed most reasonable to restrict the up-scaling experiment to this season. For all further studies of seasonality more (similar) large-scale observations are necessary to allow the generation of a transmittance seasonality for different ice types [*Nicolaus et al.*, 2010b; *Perovich et al.*, 2011]. Therefore, additional observations are suggested as future work. This would be most beneficial between May and July when fluxes are highly relevant for sea-ice mass balance and primary productivity. At that time of year, the distribution of snow is particularly important in determining light penetration and control its spatial variability [*Perovich*, 1996]. In contrast, snow effects can be neglected in the results presented here due to the general lack of snow cover. Nevertheless, light transmission and its potential variability during summer is of crucial importance due to high transmittance of sea ice (incl. melt ponds) and high solar irradiance.

4. Conclusions

[17] The results and discussion presented here strongly suggest that light transmittance and energy absorption of Arctic sea ice will increase in the future. This adds to the expected increase due to sea-ice retreat and will cause more solar heat input into the upper ocean. The main reason for this change is the greater melt-pond fraction on first-year ice compared to multi-year sea ice, and the observed trends towards younger and thinner sea ice. Our results are based on novel ROV-based radiation measurements under sea ice, combined with a new approach for Arctic-wide up-scaling, including the combined use of different satellite data sets.

References

Arrigo, K. R., G. van Dijken, and S. Pabi (2008), Impact of a shrinking Arctic ice cover on marine primary production, *Geophys. Res. Lett.*, *35*, L19603, doi:10.1029/2008GL035028.

Arrigo, K. R., et al. (2012), Massive phytoplankton blooms under Arctic sea ice, *Science*, *336*(6087), 1408, doi:10.1126/science.1215065.

Boé, J. L., A. Hall, and X. Qu (2009), September sea-ice cover in the Arctic Ocean projected to vanish by 2100, *Nat. Geosci.*, *2*(5), 341–343, doi:10.1038/ngeo467.

Comiso, J. C. (2012), Large decadal decline of the Arctic multiyear ice cover, *J. Clim.*, *25*(4), 1176–1193, doi:10.1175/JCLI-D-11-00113.1.

Ehn, J. K., C. J. Mundy, D. G. Barber, H. Hop, A. Rossnagel, and J. Stewart (2011), Impact of horizontal spreading on light propagation in melt pond covered seasonal sea ice in the Canadian Arctic, *J. Geophys. Res.*, *116*, C00G02, doi:10.1029/2010JC006908.

Eicken, H., H. R. Krouse, D. Kadko, and D. K. Perovich (2002), Tracer studies of pathways and rates of meltwater transport through Arctic summer sea ice, *J. Geophys. Res.*, *107*(C10), 8046, doi:10.1029/2000JC000583.

Eicken, H., T. C. Grenfell, D. K. Perovich, J. A. Richter-Menge, and K. Frey (2004), Hydraulic controls of summer Arctic pack ice albedo, *J. Geophys. Res.*, *109*, C08007, doi:10.1029/2003JC001989.

Fetterer, F., and N. Untersteiner (1998), Observations of melt ponds on Arctic sea ice, *J. Geophys. Res.*, *103*(C11), 24,821–24,835, doi:10.1029/98JC02034.

Frey, K. E., D. K. Perovich, and B. Light (2011), The spatial distribution of solar radiation under a melting Arctic sea ice cover, *Geophys. Res. Lett.*, *38*, L22501, doi:10.1029/2011GL049421.

Gerdes, R., and P. Lemke (2012), Sea-ice-ocean modeling, in *Arctic Climate Change*, edited by P. Lemke and H.-W. Jacobi, pp. 381–403, Springer, Dordrecht, Netherlands, doi:10.1007/978-94-007-2027-5_10.

Haas, C., A. Pfaffling, S. Hendricks, L. Rabenstein, J.-L. Etienne, and I. Rigor (2008), Reduced ice thickness in Arctic transpolar drift favors rapid ice retreat, *Geophys. Res. Lett.*, *35*, L17501, doi:10.1029/2008GL034457.

Kwok, R. (2007), Near zero replenishment of the Arctic multiyear sea ice cover at the end of 2005 summer, *Geophys. Res. Lett.*, *34*, L05501, doi:10.1029/2006GL028737.

Kwok, R., and D. A. Rothrock (2009), Decline in Arctic sea ice thickness from submarine and ICESat records: 1958–2008, *Geophys. Res. Lett.*, *36*, L15501, doi:10.1029/2009GL039035.

Light, B., T. C. Grenfell, and D. K. Perovich (2008), Transmission and absorption of solar radiation by Arctic sea ice during the melt season, *J. Geophys. Res.*, *113*, C03023, doi:10.1029/2006JC003977.

Markus, T., J. C. Stroeve, and J. Miller (2009), Recent changes in Arctic sea ice melt onset, freezeup, and melt season length, *J. Geophys. Res.*, *114*, C12024, doi:10.1029/2009JC005436.

Maslanik, J., C. Fowler, J. Stroeve, S. Drobot, J. Zwally, D. Yi, and W. Emery (2007), A younger, thinner Arctic ice cover: Increased potential for rapid, extensive sea-ice loss, *Geophys. Res. Lett.*, *34*, L24501, doi:10.1029/2007GL032043.

Maslanik, J., J. Stroeve, C. Fowler, and W. Emery (2011), Distribution and trends in Arctic sea ice age through spring 2011, *Geophys. Res. Lett.*, *38*, L13502, doi:10.1029/2011GL047735.

Nicolaus, M., and C. Katlein (2012), Mapping radiation transfer through sea ice using a remotely operated vehicle (ROV), *Cryosphere Discuss.*, *6*, 3613–3646, doi:10.5194/tcd-6-3613-2012.

Nicolaus, M., S. R. Hudson, S. Gerland, and K. Munderloh (2010a), A modern concept for autonomous and continuous measurements of spectral albedo and transmittance of sea ice, *Cold Reg. Sci. Technol.*, *62*(1), 14–28, doi:10.1016/j.coldregions.2010.03.001.

Nicolaus, M., S. Gerland, S. R. Hudson, S. Hanson, J. Haapala, and D. K. Perovich (2010b), Seasonality of spectral albedo and transmissivity as observed in the Arctic Transpolar Drift in 2007, *J. Geophys. Res.*, *115*, C11011, doi:10.1029/2009JC006074.

Pegau, W. S., and J. R. V. Zaneveld (2000), Field measurements of in-ice radiance, *Cold Reg. Sci. Technol.*, *31*(1), 33–46, doi:10.1016/S0165-232X(00)00004-5.

Perovich, D. K. (1996), The optical properties of sea ice, *Monogr. 96–1*, Cold Reg. Res. and Eng. Lab., Hanover, N. H.

Perovich, D. K. (2005), On the aggregate-scale partitioning of solar radiation in Arctic sea ice during the Surface Heat Budget of the Arctic Ocean (SHEBA) field experiment, *J. Geophys. Res.*, *110*, C03002, doi:10.1029/2004JC002512.

Perovich, D. K., and C. Polashenski (2012), Albedo evolution of seasonal Arctic sea ice, *Geophys. Res. Lett.*, *39*, L08501, doi:10.1029/2012GL051432.

Perovich, D. K., K. F. Jones, B. Light, H. Eicken, T. Markus, J. Stroeve, and R. Lindsay (2011), Solar partitioning in a changing Arctic sea-ice cover, *Ann. Glaciol.*, *52*(57), 192–196, doi:10.3189/172756411795931543.

Popova, E. E., A. Yool, A. C. Coward, F. Dupont, C. Deal, S. Elliott, E. Hunke, M. B. Jin, M. Steele, and J. L. Zhang (2012), What controls primary production in the Arctic Ocean? Results from an intercomparison of five general circulation models with biogeochemistry, *J. Geophys. Res.*, *117*, C00D12, doi:10.1029/2011JC007112.

Serreze, M. C., M. M. Holland, and J. Stroeve (2007), Perspectives on the Arctic's shrinking sea-ice cover, *Science*, *315*(5818), 1533–1536, doi:10.1126/science.1139426.

Slagstad, D., I. H. Ellingsen, and P. Wassmann (2011), Evaluating primary and secondary production in an Arctic Ocean void of summer sea ice: An experimental simulation approach, *Prog. Oceanogr.*, *90*(1–4), 117–131, doi:10.1016/j.pocean.2011.02.009.

Worby, A. P., C. A. Geiger, M. J. Paget, M. L. Van Woert, S. F. Ackley, and T. L. DeLiberty (2008), Thickness distribution of Antarctic sea ice, *J. Geophys. Res.*, *113*, C05S92, doi:10.1029/2007JC004254.